J. Fluid Mech. (1997), *vol.* 347, *pp.* 347–368. Printed in the United Kingdom

Stability of wet agglomerates in granular shear flows

By M. IRFAN KHAN AND GABRIEL I. TARDOS

Department of Chemical Engineering, The City College of The City University of New York, Convent Ave. and 140 St., New York, NY 10031, USA

(Received 16 November 1996 and in revised form 2 June 1997)

An agglomerate made of solid particles held together by a viscous liquid phase when sheared in an otherwise dry granular material is observed to deform by stretching. This observation, based on experimental results, is confirmed in the present paper by means of a computer simulation model. Simulations as well as experimental results indicate that the degree of deformation by stretching, a critical factor influencing the stability of such agglomerates, is governed by a dimensionless parameter of the system, called the deformation Stokes number, St_{def}. Two regimes, involving high and low characteristic degrees of deformation, can be identified based upon the value of this number. Simulation results indicate that for the range of conditions simulated, the value separating the two regimes, the critical deformation Stokes number, St^*_{def}, is relatively insensitive to the agglomerate size and other parameters of the system. This critical number defines the conditions below which forces inducing agglomerate breakage are low and above which they are high and result in agglomerate break-up. Calculation and/or measurement of this parameter is essential for prediction of equilibrium sizes of agglomerates in industrial granulation operations.

1. Introduction

Consider a granular material in which the interstitial fluid is a gas, except for the interstices among a few neighbouring particles which are filled with a liquid. Owing to its high viscosity and surface tension, the liquid will tend to hold these particles together and the entity will behave as a 'wet' agglomerate. Such wet agglomerates will occur spontaneously whenever a stationary or flowing powder mass comes in contact with liquid droplets, or when a liquid phase is created on the surface of particles due to high temperatures or a chemical reaction. Formation of the wet agglomerates may be undesirable, as in high-temperature fluidized beds, or desirable, as in binder granulation of powders. The present work is motivated mainly by the latter problem.

In binder granulation, fine powdery particles are agglomerated into larger granules in order to improve properties like bulk density, flowability, dispensability and to reduce dustiness. For a mixture of different powder types, such as in many pharmaceutical formulations, granulation provides resistance against component segregation. Many food products are granulated in order to have pleasant appearance and good 'instant' properties such as wettability, sinkability, dispersibility and solubility. Agglomeration in binder granulation is carried out by spraying onto a moving powder mass a binder liquid to yield wet agglomerates. Movement in the powder mass is induced by an apparatus such as a rotating drum, fluidized bed or a high-shear mixer. Local conditions of shear in the moving powder mass serve to induce both coalescence

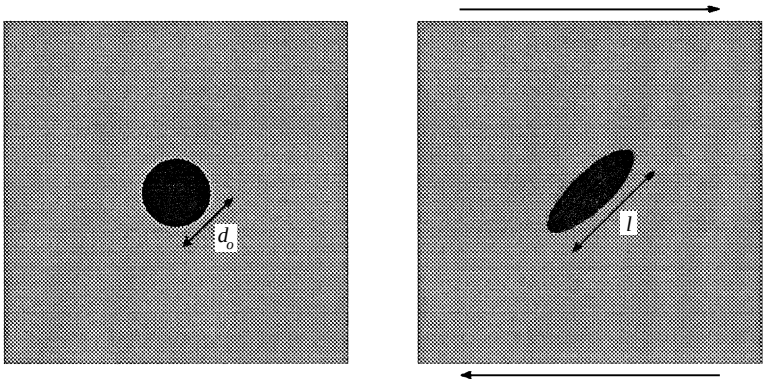

FIGURE 1. A wet agglomerate in a granular medium which is (*a*) stationary and (*b*) sheared.

as well as breakage of wet agglomerates and hence define a steady agglomerate size. Wet agglomerates are subsequently dried to yield the final product in which particles are bound together by solid bridges left behind by the binder fluid.

A major issue in modelling of such a process is the influence of operating parameters, such as particle and binder fluid properties and the magnitude of imposed shear, on the steady-state size of agglomerates. Operating parameters influence the steady-state size of agglomerates by generating forces that induce coalescence and breakage. While the influence of the phenomenon of agglomerate coalescence has been researched in the past, the influence of the equally important phenomenon of agglomerate breakage lacks serious exploration (Simons 1996). The primary reason is that agglomerate breakage by its very nature is quite an unpredictable phenomenon, not easily analysed by conventional analytical tools. The present study is an attempt to analyse the phenomenon of agglomerate deformation and breakage, which is induced as a result of shear forces in the surrounding dry particulate medium.

2. Problem formulation

The problem to be analysed is depicted schematically in figure 1. An initially spherical wet agglomerate in a stationary granular medium (figure 1*a*), starts deforming by stretching when the surrounding granular medium is sheared (figure 1*b*). This behaviour has been observed in the presented experimental results (see §5), where a shear field of granular solids is created in a fluidized bed Couette device, and the response of wet agglomerates in this shearing granular medium is studied. Experimental results indicate that if the degree of deformation exceeds a particular limit, wet agglomerates become susceptible to breakage. The degree of deformation depends on system parameters such as the properties of the wet agglomerate, those of the granular medium and upon the imposed shear rate. In the present work we aim to evaluate this dependence by means of a computer simulation model, and subsequently compare the results with those obtained from experiments.

The force inducing deformation of the agglomerate in figure 1 is the inertial force due to the surrounding granular medium. The force resisting its deformation is the viscous drag opposing the movement of individual particles in it. The ratio of these two forces (inducing to resisting) can be expected to govern the dynamics of deformation of the agglomerate. Tendency towards deformation (and hence breakage) should be large for large values of this ratio and vice versa. The ratio of particle

inertia to the viscous drag has been referred to in the literature as the Stokes number (Koch 1990; Ennis, Tardos & Pfeffer 1991). We have hence termed this ratio the deformation Stokes number, St_{def}, which can be written as

$$St_{def} = \frac{\rho_{p_g} U_g^2}{\mu U_a / d_{p_a}}. \tag{1}$$

The numerator in the above expression represents the characteristic inertial force in the surrounding granular medium, where ρ_{p_g} and U_g are particle density and its characteristic velocity, respectively. The denominator represents the characteristic viscous force in the agglomerate, induced as a result of a particle moving relative to the interstitial fluid with a characteristic velocity U_a in the Stokes flow regime, where μ is the viscosity of the interstitial fluid and d_{p_a} is the diameter of a particle within the agglomerate phase. If $\dot{\gamma}$ is the imposed shear rate, a characteristic particle velocity in the agglomerate phase is $d_{p_a}\dot{\gamma}$, while that in the granular phase is $d_{p_g}\dot{\gamma}$, where d_{p_g} is the diameter of a particle within the granular phase. The expression for St_{def} then simplifies to

$$St_{def} = \frac{\rho_{p_g} d_{p_g}^2 \dot{\gamma}}{\mu}. \tag{2}$$

As a measure of the degree of deformation (by elongation) of the agglomerate, we introduce the elongation parameter, E, defined as

$$E = \frac{l}{d_o} \tag{3}$$

where d_o is the diameter of the original undeformed (spherical) agglomerate and l the major axis of the deformed one (figure 1). The range of experimentally observed values of E lies between 1 (for zero deformation) and 1.5 (for highly deformed agglomerates). E can be used as a measure of the agglomerate's tendency towards breakage. Low values of E would imply a low tendency towards breakage and vice versa. The objective of analysing the present problem then reduces to correlating E with St_{def}.

3. The computer simulation model

A computer simulation model is developed to analyse the above problem. The model is based on the discrete element approach for simulating flows of a granular material, and of a suspension of particles. The two approaches, applied separately in the granular or the external phase, and the agglomerate or the interior phase, are discussed further in the following two subsections.

3.1. *Granular phase*

Particles in the granular phase are modelled as smooth rigid spheres of uniform size. The interstitial fluid is assumed to be of very low density and viscosity (such as air), so that it plays no significant part in momentum transfer. Particle trajectories between successive collisions can then be approximated by Newton's equation of motion. A computer simulation of the flow of such particles computes trajectories between two successive collisions and modifies them appropriately during a collision by satisfying the conservations of linear/angular momentum and energy. The inter-particle interactions during a collision are usually characterized by two parameters: the coefficient of restitution, e (the ratio of approach to recoil velocities), and the

coefficient of surface friction, σ. Both these parameters are usually taken as constant particle properties. In the present simulations the only parameter of interest is e, since the particles are considered to be smooth on their outer surface.

There are several such simulations in the literature. Existing simulation techniques mainly differ from one another in the manner in which they satisfy the conservation of linear/angular momentum and energy during a collision, and upon the definition of conditions under which a collision is assumed to occur. These techniques can be broadly classified into three main types (Hopkins & Louge 1990): hard-particle collision, soft-particle contact and hard-particle overlap models. The hard-particle collision model assumes the particles to be hard spheres and hence a collision is assumed to occur instantly upon contact. During a collision the colliding particle pair undergoes an instantaneous change in its linear/angular momentum, the change being a function of the coefficients of restitution and surface friction. The model progresses in time by searching for the most imminent collision in the system (the closest point in time at which any two particles in the system just touch), moving the system to the point of this collision, and then executing the collision. In soft-particle contact model the particles are modelled as deformable on their outer surface. The simulation proceeds by moving the system ahead over small predetermined time intervals after which the particles overlap slightly. The overlaps are interpreted as deformations and a repulsive force based on a spring and dashpot model is generated. The properties of this model are chosen such that the collision outcome is consistent with the chosen values of e and σ. The hard-particle overlap model combines the above two approaches by modelling particles as rigid spheres while also allowing for an overlap. The simulation proceeds over small time intervals, after each one of which the overlaps between particles are checked and a collision is executed whenever one is detected. The time interval is kept low enough so that on an average only a very tiny fraction (say 1%) of the particle diameter is overlapped and the system properties such as the stresses in the flow become independent of a further reduction in the time interval. Each model is suitable for simulating flows in a particular density range: hard-particle collision model at low density, soft-particle contact at high density and hard-particle overlap model in the intermediate density range. In the current problem we deal with flows in the intermediate density range and hence we have used the hard-particle overlap model, developed by Hopkins & Louge (1990), in the present simulations.

For computational efficiency we have simulated the flow of spheres, the motion of which is restricted to lie in a plane. While an idealization, this type of flow has been regarded as a good approximation for three-dimensional shear flows of granular materials as well as that of suspensions, since the pair distribution functions in the two cases are expected not to differ significantly from one another (Bossis & Brady 1984). Experiments with such systems, involving granular materials (Aidanpää, Shen & Gupta 1996) as well as suspensions (Bouillot *et al.* 1982), have also been performed. This shows that these types of flows are also practically realizable. The simulation domain along the plane of particle movement is rectangular with horizontal and vertical edge dimensions equal to L_x and L_y respectively. The domain is surrounded on all four sides by mirror images as is shown in figure 2. If image boxes at the top are moved in the x-direction with a velocity v and those at the bottom moved in the $-x$-direction with a velocity $-v$, the simulation domain experiences a constant shear rate equal to v/L_y. This is called a periodic boundary condition and has been used widely for simulating shear flow of a granular material (Walton & Braun 1986; Campbell 1989; Hopkins

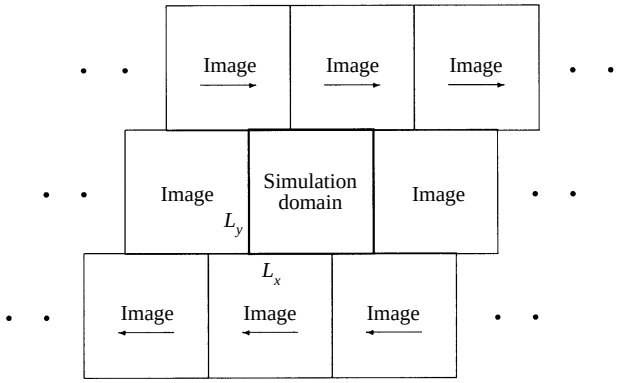

FIGURE 2. Simulation of a shear flow of particles in a domain following a periodic boundary condition.

Conditions			Hopkins & Louge			Present simulations		
ν	e	L/d_p	τ_{11}	$\tau_{12}=\tau_{21}$	τ_{22}	τ_{11}	$\tau_{12}=\tau_{21}$	τ_{22}
				Kinetic stresses				
0.3	0.9	83	1.605	−0.420	1.374	1.673	−0.411	1.381
0.5	0.9	83	1.201	−0.264	1.119	1.302	−0.262	1.141
0.6	0.9	83	1.222	−0.222	1.166	1.361	−0.222	1.196
				Collisional stresses				
0.3	0.9	83	1.522	−0.358	1.447	1.576	−0.379	1.496
0.5	0.9	83	3.500	−0.973	3.415	3.664	−1.012	3.567
0.6	0.9	83	6.352	−1.829	6.233	6.759	−1.951	6.648

TABLE 1. A comparison of the data for stresses in flow in the present simulations in the absence of an agglomerate with those in Hopkins & Louge (1990)

& Louge 1990). In addition, for providing a means of conserving particles in the simulation domain, a periodic boundary condition provides an approximation to simulating a domain which is a part of an infinite region undergoing uniform shear flow.

For most part, the present simulation of granular phase is similar to that of Hopkins & Louge (1990). Table 1 is a comparison of the data for their steady state stresses in the flow with that in the present simulation in the absence of an agglomerate. Good agreement with their data (within 5% in most cases) is observed. The data correspond to the simulation of smooth spherical two-dimensional disks of uniform size in a square domain with an edge dimension equal to L. In table 1 ν denotes the solid fraction, e the coefficient of restitution, and L/d_p the ratio of the edge dimension L to the particle diameter d_p. The upper half of the table is a comparison for the kinetic component of the stress tensor, $\boldsymbol{\tau}_k$, which represents the momentum transfer due to the motion of particles between collisions, and the lower half is a comparison for the collisional component, $\boldsymbol{\tau}_c$, which represents the momentum transfer due to interparticle collisions. The overall stress tensor, $\boldsymbol{\tau}$, is equal to $\boldsymbol{\tau}_k + \boldsymbol{\tau}_c$. For details on computations of $\boldsymbol{\tau}_k$ and $\boldsymbol{\tau}_c$ in the simulation model and for a further elaboration on the simulation in the granular phase, refer to Hopkins & Louge (1990).

3.2. *Agglomerate phase*

In the present work a 'wet agglomerate' phase has been introduced in the centre of the simulation domain. In this phase the interstitial fluid is relatively dense and viscous (such as water or an organic binder fluid used in industrial granulation operations). The contribution of the interstitial fluid in momentum transfer cannot be ignored now. The resulting particle movement can be modelled by an approach known as Stokesian Dynamics (Brady & Bossis 1988). In its most general form the particle motion in a fluid is modelled by the Langevin equation:

$$\boldsymbol{m} \cdot \frac{\mathrm{d}\boldsymbol{U}}{\mathrm{d}t} = \boldsymbol{F}^H + \boldsymbol{F}^P + \boldsymbol{F}^B, \tag{4}$$

where $\boldsymbol{m}$ is the generalized mass/moment-of-inertia matrix, $\boldsymbol{U}$ is the particle velocity vector, $\boldsymbol{F}^H$ is a vector of hydrodynamic force exerted on particles due to their motion relative to the fluid, $\boldsymbol{F}^P$ is the vector of deterministic non-hydrodynamic forces which may be interparticle ($\boldsymbol{F}^I$) or external ($\boldsymbol{F}^E$), and $\boldsymbol{F}^B$ is the vector of the stochastic forces that give rise to Brownian motion. For a suspension of particles of size greater than a micron in ordinary fluids such as water or air under normal conditions of temperature and pressure, $\boldsymbol{F}^B$ provides a negligible correction to particle velocity in equation (4). Under the assumption that the contribution of $\boldsymbol{F}^B$ is negligible, that the external forces such as gravity are absent and that all particles are identical, spherical and smooth on their outer surface, (4) reduces to

$$m_p \frac{\mathrm{d}\boldsymbol{U}}{\mathrm{d}t} = \boldsymbol{F}^H + \boldsymbol{F}^I, \tag{5}$$

where m_p is the particle mass and $\boldsymbol{F}^I$ represents the interaction forces between particles. We model the interparticle interactions in the same manner as in the granular phase, i.e. the particles are taken as hard spheres having a constant coefficient of restitution which interact impulsively during a collision. Hence the particle motion between collisions follows the equation

$$m_p \frac{\mathrm{d}\boldsymbol{U}}{\mathrm{d}t} = \boldsymbol{F}^H. \tag{6}$$

Two important dimensionless parameters can be identified in the agglomerate phase. The particle Reynolds number (Re_p) is the ratio of fluid inertia to drag force due to the particle motion:

$$Re_p = \frac{\rho_{f_a} d_{p_a} U_a}{\mu} = \frac{\rho_{f_a} d_{p_a}^2 \dot{\gamma}}{\mu}, \tag{7}$$

where ρ_{f_a} is the interstitial fluid density in the agglomerate and the characteristic particle velocity in the agglomerate phase, U_a, is again taken as $d_{p_a}\dot{\gamma}$. The particle Stokes number (St_p) is the ratio of particle inertia to the drag force experienced by it and hence can be expressed as

$$St_p = \frac{\rho_{p_a} U_a^2}{\mu U_a / d_{p_a}} = \frac{\rho_{p_a} d_{p_a}^2 \dot{\gamma}}{\mu}. \tag{8}$$

St_p is thus simply related to Re_p as $St_p = (\rho_{p_a}/\rho_{f_a})Re_p$, and to the deformation Stokes number, St_{def}, defined in equation (2) as $St_p = (\rho_{p_a} d_{p_a}^2/\rho_{p_g} d_{p_g}^2)St_{def}$. If the particles in the granular and agglomerate phase are identical, St_p is equal to St_{def}.

If $Re_p \ll 1$, the hydrodynamic force induced by the particles on the fluid, $-\boldsymbol{F}^H$, is related to the particle velocity $\boldsymbol{U}$ by the following linear relation (Happel & Brenner 1973):

$$-\boldsymbol{F}^H = \boldsymbol{R}(\boldsymbol{x})(\boldsymbol{U} - \boldsymbol{U}^\infty), \tag{9}$$

where $\boldsymbol{U}^\infty$ is the fluid velocity in the absence of particles (and is equal to zero in the present case), and $\boldsymbol{R}$ is the resistance matrix, which depends only on the particle configuration $\boldsymbol{x}$. The Langevin equation (6) then reduces to

$$St_p \frac{\mathrm{d}\hat{\boldsymbol{U}}(\hat{t})}{\mathrm{d}\hat{t}} = -18\hat{\boldsymbol{R}}(\boldsymbol{x})\hat{\boldsymbol{U}}(\hat{t}), \tag{10}$$

where the hats represent non-dimensional variables. Here $\boldsymbol{U}$ is non-dimensionalized by $\dot{\gamma}\, d_{p_a}$, t by $\dot{\gamma}^{-1}$ and the resistance matrix, $\boldsymbol{R}$, by the drag factor $3\pi\mu d_{p_a}$. We wish to model the particle movement in the agglomerate by (10) expressed in a finite difference form. If the time step of integration is kept small enough, $\boldsymbol{R}$ can be approximated by the identity matrix $\boldsymbol{I}$ since $\boldsymbol{R}$ is computed as a function of the particle configuration $\boldsymbol{x}$ at each step (Ichiki & Hayakawa 1995). Under this approximation (10) simplifies to

$$\hat{\boldsymbol{U}}(\hat{t}) = \hat{\boldsymbol{U}}(0)\exp\left(-\frac{18\hat{t}}{St_p}\right). \tag{11}$$

From (11) it is apparent that St_p is an important parameter governing the dynamics of particle movement in the agglomerate. When particles come very close to one another, short-range lubrication forces become important and the present scaling of $\boldsymbol{R}$ breaks down. The present simulation does not capture this effect and neglects the presence of the lubrication forces. However, as an approximation, we have taken the coefficient of restitution in the agglomerate phase as zero in an attempt to incorporate the effect of relatively large lubrication forces.

Since the agglomerate phase is freely suspended in the granular phase, the agglomerate as a whole will translate and rotate relative to the granular phase. The particle velocity vector in the agglomerate phase with respect to a fixed reference frame is thus

$$\boldsymbol{U} = \boldsymbol{U}^A + \boldsymbol{U}^R, \tag{12}$$

where $\boldsymbol{U}^A$ is the velocity of the agglomerate as a whole with respect to the fixed reference frame and $\boldsymbol{U}^R$ is the particle velocity in the agglomerate with respect to a reference frame fixed to the agglomerate. It is $\boldsymbol{U}^R$ that contributes to the Stokesian Dynamics calculations. The agglomerate velocity, $\boldsymbol{U}^A$, can be computed from the force/torque balance on the agglomerate. It can be written as $\boldsymbol{U}^A = \boldsymbol{U}^A_T + \boldsymbol{U}^A_R$, where $\boldsymbol{U}^A_T$ is the translational and $\boldsymbol{U}^A_R$ is the rotational component. The translational component, $\boldsymbol{U}^A_T$, can be evaluated by considering the force balance:

$$m_a \frac{\mathrm{d}\boldsymbol{U}^A_T}{\mathrm{d}t} = \sum_i \boldsymbol{F}^H_i, \tag{13}$$

where m_a is the mass of the agglomerate and can be estimated by modelling the agglomerate as having no interstitial fluid and having particles possessing an 'effective enhanced mass', $\hat{m}_p$, due to the presence of interstitial fluid. $\hat{m}_p$ can be estimated as

$$\hat{m}_p = \left(1 + \frac{\rho_{f_a}}{\rho_{p_a}}\left(\frac{1 - v_a}{v_a}\right)\right) m_p = \beta\, m_p, \tag{14}$$

where v_a is the solid fraction in the agglomerate and β is called the mass enhancement

factor. The agglomerate mass, m_a, is then equal to $N_a \hat{m}_p$, where N_a is the total number of particles in the agglomerate. The rotational component of agglomerate velocity, $\boldsymbol{U}_R^A$, can be evaluated by considering the torque balance:

$$I_a \frac{\mathrm{d}\boldsymbol{\omega}}{\mathrm{d}t} = \sum_i \tilde{\boldsymbol{r}}_i \times \boldsymbol{F}_i^H, \tag{15}$$

where I_a is the moment of inertia, $\boldsymbol{\omega}$ the angular velocity and $\tilde{\boldsymbol{r}}_i$ the position vector with respect to the centre of mass of the agglomerate, and $\times$ denotes the vector cross-product. The moment of inertia of the agglomerate, I_a, can be estimated as

$$I_a = \sum_i \hat{m}_p \, (\tilde{\boldsymbol{r}}_i \cdot \tilde{\boldsymbol{r}}_i). \tag{16}$$

The rotational component of agglomerate velocity, $\boldsymbol{U}_R^A$, can then be computed as $\boldsymbol{\omega} \times \tilde{\boldsymbol{r}}_i$.

We now examine the effect of surface tension forces experienced by the particles at the outer surface of the agglomerate. Such forces, if significant, would tend to influence the deformed state of the agglomerate even when the forces inducing its deformation are absent (as in the case of a liquid drop which tries to regain its original spherical shape as soon as the forces inducing its deformation cease to exist). However, simple laboratory experiments show that a deformed wet agglomerate has no tendency to alter its state in the absence of forces inducing its deformation. We hence conclude that surface tension forces do not play a significant role in governing the dynamics of particle movement in the agglomerate and hence have neglected their effect in the present simulation.

We now examine the assumption $Re_p \ll 1$ by making an estimate of its highest possible order of magnitude under practical conditions. A typical large shear rate employed in a granulation apparatus is of the order 10^2 s^{-1}. Taking an approximation of the largest particle size of powders granulated as 100 μm and taking the interstitial fluid to be at the low end on the viscosity scale, such as water for example, we estimate the value of Re_p from equation (7) as 1. Most processes however, would employ lower shear rates, use binder fluids more viscous than water and granulate powders with a mean size of less than 100 μm. Hence we conclude that the assumption $Re_p \ll 1$ would be met under most practical conditions.

4. Simulation results

Parameters chosen for the present simulation, except for the deformation Stokes number, St_{def}, are given in table 2. Figure 3 is a picture of the simulation domain as it looks initially. Since particles are taken as spheres, the motion of which is restricted to lie in a plane, figure 3 provides a view which is normal to the plane containing these particles. The dark coloured particles in the centre represent the agglomerate, while the rest form the granular phase. Since particles in the granular and agglomerate phases are taken as identical, St_{def} is equal to St_p. Initial solid fraction (fraction of space occupied by solids in the plane containing the center of particles) in the agglomerate phase is set at the maximum value which can be sheared homogeneously in two dimensions, $\pi/4$ or 0.785 (Brady & Bossis 1985). This high initial value is necessary to avoid an excessive 'capture' of particles from the granular phase during the course of the simulation. Initial solid fraction in the granular phase is taken as 0.65. Initial particle positions follow a regular square lattice arrangement

Quantity	Value	Comments
L_x	1	Horizontal edge dimension of the simulation domain
L_y	1	Vertical edge dimension of the simulation domain
N	10 000	Number of particles simulated
v_g	0.65	Solid fraction in the granular phase
v_a	0.785	Solid fraction in the agglomerate phase
e_g	0.5	Coefficient of restitution in the granular phase
e_a	0.0	Coefficient of restitution in the agglomerate phase
α	2.0	Particle to fluid density ratio in the agglomerate
d_{pg}	0.009127	Diameter of particles in the granular phase
d_{pa}	0.009127	Diameter of particles in the agglomerate phase
d_a	0.20	Diameter of the agglomerate
f	0.02	Set point for average fraction of particle dia. overlapped

TABLE 2. Conditions for simulation corresponding to figures 3–6, 8 and 9. The only input parameter changed in these figures is the deformation Stokes number, St_{def}

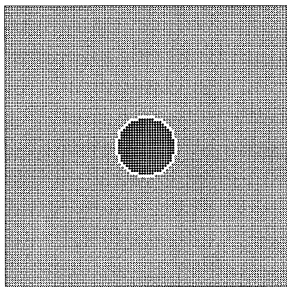

FIGURE 3. Snapshot of the simulation domain at zero dimensionless time units for conditions listed in Table 2.

and the centre of mass of the system coincides with the centre of the simulation domain. Particle velocities in the granular phase are initialized as the mean shear velocity superimposed on a small random component, in order to initiate collisions. Particle velocities in the agglomerate phase are initialized as zero. Initial particle velocities are readjusted slightly so that the initial net momentum of the domain is zero.

As the simulation is allowed to proceed in time the agglomerate phase moves relative to the granular phase and at times tends to come close to, or worse leave, the boundary of the domain. Since the image boundary conditions strictly hold only for a unidirectional flow (as would be the case in the absence of the agglomerate), the agglomerate must be kept as close to the centre of the domain as possible so that the disturbance in the flow field created by its presence is not felt strongly at the top and bottom edges of the domain and the flow close to these boundaries is close to being unidirectional. In the present simulations the centre of mass of the agglomerate is always kept at the centre of the domain by making small adjustments to the overall momentum of the domain at each time step. Such an adjustment at each step in effect amounts to moving the 'window' of the domain (which is used to observe the agglomerate in a region of infinite shear) such that the centre of mass of the agglomerate occupies the centre of the domain and thus should not affect any statistics or other results of the simulation except for the net momentum of the

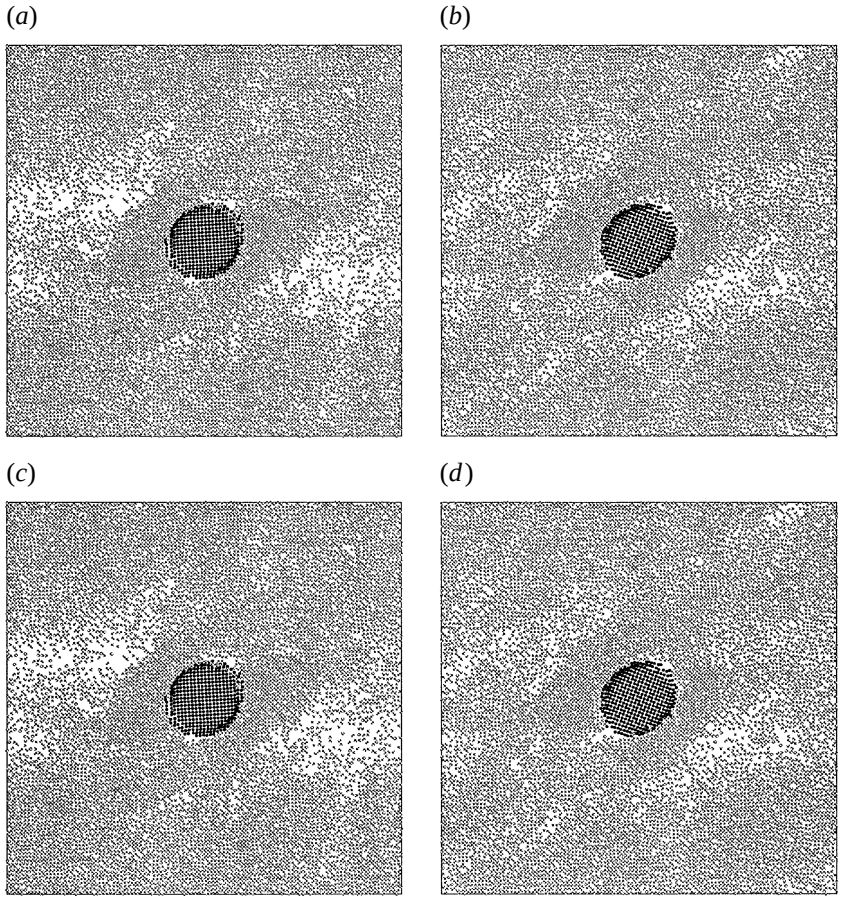

FIGURE 4. Snapshots of the simulation domain at (*a*) 25, (*b*) 50, (*c*) 75 and (*d*) 100 dimensionless time units for conditions listed in table 2 and $St_{def} = 0.018$.

domain (which remains close to zero as a result of such an exercise). This conclusion has been verified by means of a few preliminary simulations.

Figures 4 and 5 show the time evolution of the domain for cases when St_{def} is equal to 0.018 and 0.18 respectively. The time in these figures is non-dimensionalized by multiplying with the shear rate. In figure 4, where St_{def} is relatively low, the agglomerate elongates very little within 100 dimensionless time units. An increase in St_{def} by an order of magnitude in figure 5, however, produces an appreciable deformation within this time. This result is in good agreement with experimental results (see the next section) where a similar pattern of increase in the degree of elongation of agglomerates within a given time was observed as St_{def} of the system was increased. The experimental results also indicated that the deformed agglomerates become susceptible to breakage if the degree of elongation exceeds a particular value. Breakup of agglomerates occurs because at high elongations some particles are held together only by a few liquid bridges, which eventually rupture when stretched beyond a certain limit. Capturing this in a simulation would require the introduction of an appropriate rupture distance of a liquid bridge connecting two particles, and could be modelled based on an approach such as that described in Simons, Seville & Adams (1994). The situation will be complicated however by the fact that the domain will

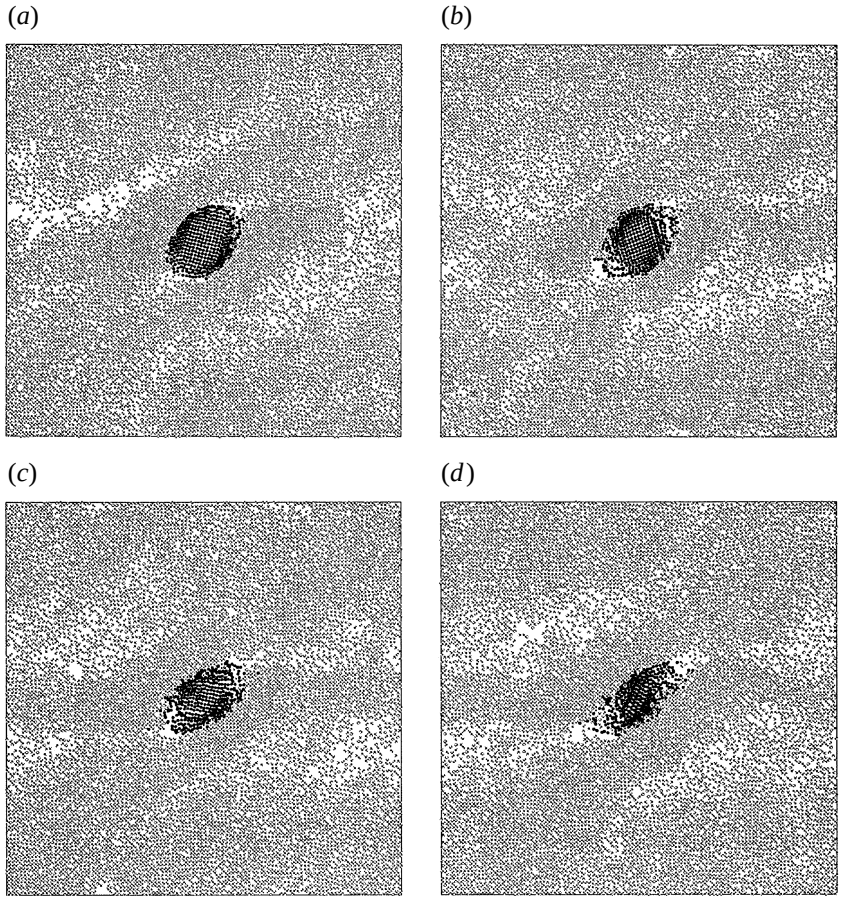

FIGURE 5. As figure 4 but for $St_{def} = 0.18$.

then contain wet particles which are not confined within a single agglomerate phase. The present simulation, hence, does not incorporate the phenomenon of liquid bridge rupture, and does not capture the phenomenon of agglomerate breakup into smaller pieces. However, by looking at the simulation domain, one can crudely judge if an agglomerate exists in a fractured state. For example, the last case in figure 5 suggests that particles are chipped off at the two edges of the elongated agglomerate.

Figure 6 provides some insight into the mechanism of agglomerate deformation. Figure 6(*a*) is a plot of the number of rotations of the agglomerate versus dimensionless time, t^*, (real time multiplied by the shear rate) for conditions listed in table 2 and St_{def} equal to 0.018 (the rotation in the agglomerate is different from a pure solid body type rotation since an elongatory motion is simultaneously present). It can be concluded from this figure that the agglomerate rotates steadily with time, completing about 2 rotations in 150 dimensionless time units. The rate of rotation shows a slight decrease with time, a phenomenon that can be understood by considering figure 7. This figure simply illustrates that a pure shear is composed of one half pure vorticity and one half pure strain. While a spherical agglomerate responds well to vorticity and rotates faster, an elongated one rotates slower and hence the decrease in the rotation rate as time progresses or as the agglomerate becomes more and more elongated. Figure 6(*b*) is a plot of the orientation of the major axis (defined

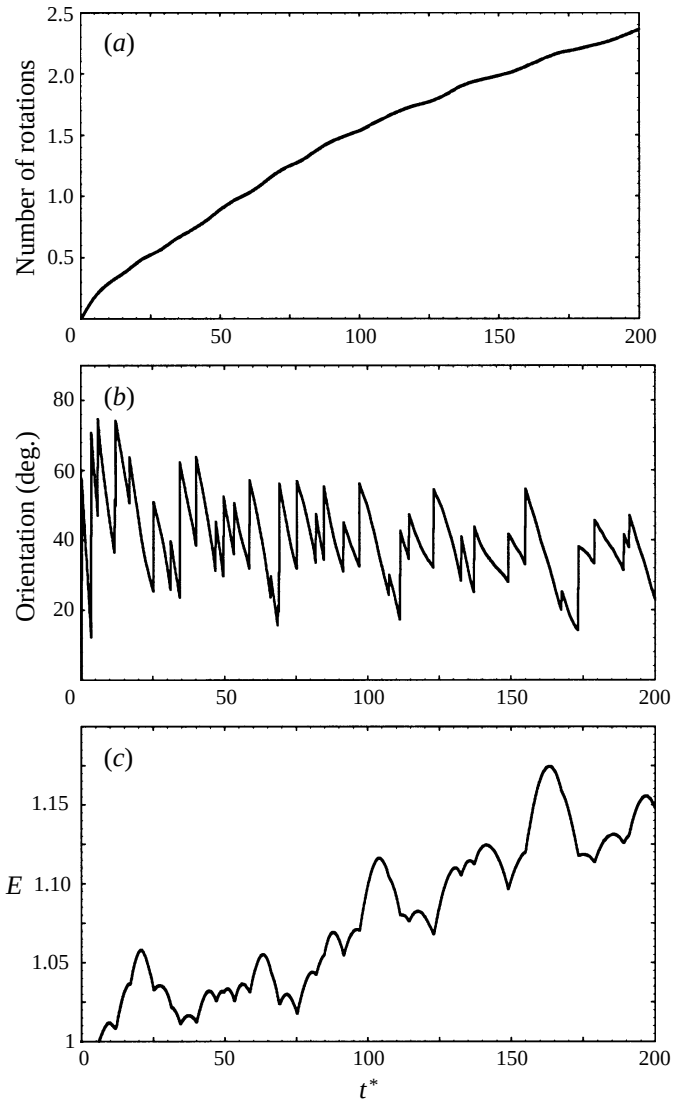

FIGURE 6. (*a*) Number of rotations of the agglomerate. (*b*) Orientation of the major axis of the deformed agglomerate. (*c*) Elongation parameter E versus the dimensionless time, t^*, for conditions listed in table 2 and St_{def} equal to 0.018.

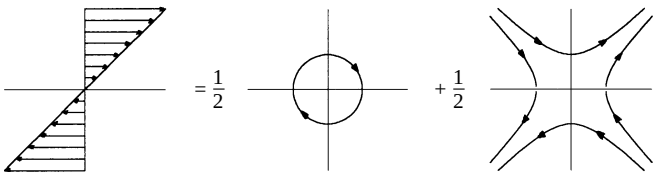

FIGURE 7. A pure shear field is composed of one-half pure vorticity and one-half pure strain.

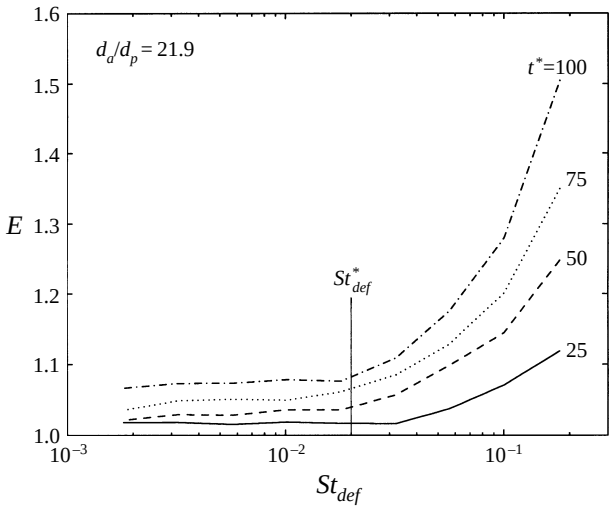

FIGURE 8. A plot of the elongation parameter, E, versus the deformation Stokes number, St_{def}, for the conditions listed in table 2 and for different values of dimensionless time units.

as the line joining the centres of the particle pair farthest away from one another in the agglomerate) of the deformed agglomerate in degrees versus dimensionless time, where the angle is measured from the positive x-direction in a counter-clockwise direction. The orientation oscillates about a mean value of approximately 45°, indicating that the elongated agglomerate tries to align itself in the direction of the straining component of the shear field (figure 7). The nearly vertical jumps in figure 6(*b*) can be attributed to the sudden appearance of a particle pair forming a new major axis at an orientation angle greater than the current. The new major axis between these particle pairs then rotates slightly with time (indicated by the slanted portions of the oscillations), decreasing the orientation until the sudden appearance of a new major axis. The period of oscillation also decreases with time indicating that elongated agglomerates have a greater tendency towards a sustained alignment in the direction of strain and a reduced tendency towards rotation than the more spherical ones, a conclusion that was also arrived at previously from observations of figure 6(*a*). Figure 6(*c*) is a plot of the elongation parameter E versus dimensionless time and shows that E increases with time, though not monotonically. The points of discontinuity in slope coincide exactly with the points of sudden jumps in figure 6(*b*), indicating that these are caused by the appearance of new particle pairs forming the major axis. As the agglomerate rotates, the major axis first increases in magnitude, which corresponds to the increasing portions of the plot in figure 6(*c*), and then decreases slightly, indicated by the decreasing portion. This decrease continues until the distance between another particle pair becomes large enough to become the new major axis. Over large time intervals E increases with time and the rate of elongation also increases, which again can be attributed to an increased response of an elongated agglomerate to the straining component of the shear field.

Figure 8 is a plot of the elongation parameter, E, versus St_{def} for conditions listed in table 2, and for different dimensionless time units. Each curve in figure 8 is formed by joining nine points obtained from several simulation results. Each point is itself an average of three obtained from different initial conditions. This averaging over

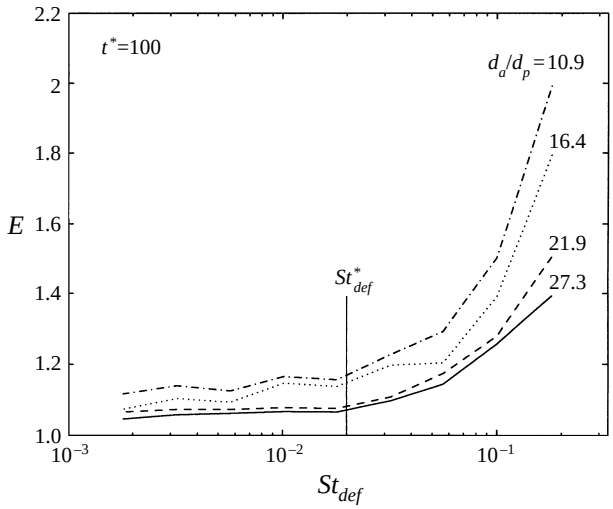

FIGURE 9. A plot of the elongation parameter, E, versus the deformation Stokes number, St_{def}, for the conditions listed in table 2 and 100 dimensionless time units for different values of relative agglomerate diameters (d_a/d_p).

several points reduces the jagged nature of the plot and makes it smoother since it in effect serves to reduce the error in the simulation. E is observed to increase with St_{def} as expected, for all times. An interesting feature of figure 8 is the existence of two distinct regimes based on the value of St_{def} having relatively low and high characteristic values of E. We call the value of St_{def} which separates these two regimes the critical deformation Stokes number, St^*_{def}. The magnitude of St^*_{def} can be concluded from figure 8 to be approximately 0.02. Since the rate of elongation for regions above St^*_{def} is significantly higher than that below, we can say that the agglomerates possess a much higher tendency towards deformation (and breakage) if the value of St_{def} lies above St^*_{def}. Thus St^*_{def} can be regarded as an important parameter characterizing the stability of the agglomerate, which, as seen from the figure, is also relatively insensitive to variation in time for the simulated dimensionless time of 100 units.

We now explore the effect of changing the agglomerate diameter relative to the particle diameter on the simulation results. Figure 9 is a plot of E versus St_{def} for conditions listed in table 2 and 100 dimensionless time units for different values of the relative agglomerate diameters (d_a/d_p). Each curve is again obtained by joining nine points obtained from simulation results, each point itself being an average of three obtained from different initial conditions. The curve for small agglomerates is a little jagged since the error in the simulation results decreases with the number of particles, N, as $1/N^{-1/2}$ (since the standard deviation of a collection of random variables decays with the sample size, N, as $1/N^{-1/2}$) and smaller agglomerates contain fewer particles. The different values of (d_a/d_p) tested were 27.34, 21.91, 16.45 and 10.98. It is apparent from this figure that, for the range of (d_a/d_p) simulated, the value of St^*_{def} is nearly insensitive to variations in the relative agglomerate size, i.e. all agglomerates make a transition from the low to high elongation regime at nearly the same value of the critical St_{def} of approximately 0.02. However, for any given value of St_{def}, agglomerates having lower relative sizes possess a higher value of E. In other words, under similar conditions smaller agglomerates tend to be more unstable

than larger ones. This relatively unstable nature of smaller agglomerates might be the reason behind the difficulty in obtaining stable nuclei (small agglomerates) during granulation (Pietsch 1996).

5. Experiments

In order to test the conclusions reached from simulation results, experiments on deformation and breakup of agglomerates were performed. The primary requirement for such an experimental study is a setup in which a granular material can flow in a manner closely approximated by simple shear flow. For Newtonian fluids, the most common arrangement of this kind is a Couette device, which consists of two concentric rotating cylinders with fluid in the annulus; the thickness of annular gap being much smaller than the diameter of cylinders. Although granular materials do not behave as Newtonian fluids, and exhibit complex flow behaviour (Campbell 1990), an 'idealized' granular material in a zero gravity environment obeying no-slip boundary conditions at the walls develops a linear velocity profile along the shear gap. This behaviour has been observed in computer simulations by Campbell & Brennen (1985). The idealized granular material used by these authors was one in which all particles were spherical, of equal size, having constant coefficients of restitution and surface friction, and which interacted only by means of instantaneous collisions. Such interparticle interaction is likely to be predominant in a real granular material when it flows fast, as in the 'grain-inertia' regime.

A common experimental technique with granular materials to obtain a no-slip boundary condition is to make the solid walls extremely rough (Savage & Syed 1984). A simple way to obtain an approximately uniform shear flow of a granular material might then be to roughen the walls of a Couette device with sandpaper of appropriate coarseness and then shear the material inside the annular gap. Such an exercise, however, would prevent the granular material from flowing in the grain-inertia regime, due to the presence of gravity (which acts along the axis of the cylinders), which increases the frictional interaction among adjacent layers in the direction of gravity. This frictional loading increases vertically down from the free surface of the granular material. This undesirable effect was eliminated in the present experiments by means of fluidizing the particles (Kunii & Levenspiel 1991) with air entering the bottom of Couette device. If the velocity of upflowing air is kept equal to the minimum fluidization velocity of particles, the upward drag force on particles balances the downward force of gravity. The net force on individual particles is then zero, and frictional interaction among them is considerably reduced. The particles can then flow in the grain-inertia regime, provided that enough momentum is imparted to them by the moving walls. The detailed experimental setup utilized in this work is shown in figure 10.

Experiments were performed with the fluidized-bed Couette device described above using glass particles of a mean size of about 300 microns such that 80% of the particles lay within the range of 350–250 microns. The density of particles was within the range of 2.42–2.5 g cm^{-3}. Under Geldart's classification scheme (Kunii & Levenspiel 1991), these particles classify as class B. The minimum fluidization velocity of the particles was found experimentally to be about 8 cm s^{-1}. The volume fraction of bed at minimum fluidization conditions was estimated approximately as 0.4 (Kunii & Levenspiel 1991). Sandpaper was glued to the walls of the two cylinders as shown in figure 10. Its coarseness was chosen such that it was roughly equal to the size of glass beads. The bed was fluidized at minimum fluidization conditions and the inner

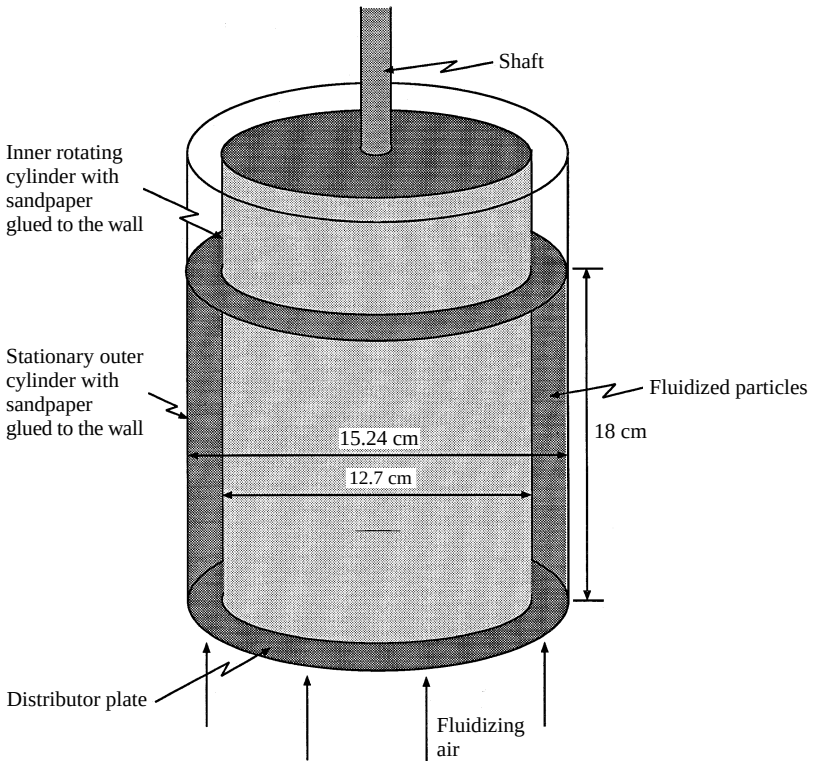

FIGURE 10. Schematic of the fluidized-bed granular-flow Couette device.

cylinder rotated. Rotation at low speeds caused shear only in the particles close to the inner rotating cylinder. This was due to the fact that granular flows dissipate energy, and hence energy imparted by the moving wall had to exceed a certain threshold in order to cause flow across the gap. Shear penetrated the whole bed only for rotational speeds exceeding about 50 RPM. High rotation speeds (exceeding about 100 RPM) caused slip on the inner wall, due to a decrease in 'particle pressure', caused by an increase in the centrifugal forces experienced by the particles. Hence, in all experiments, the rotational speed of the inner cylinder had to be kept between 50 and 100 RPM. The shear rate in the annular gap was estimated from the velocity of the inner cylinder and the thickness of the shear gap.

Wet agglomerates were formed in the Couette device kept at minimum fluidization conditions by adding droplets of an aqueous solution of 20 K Carbowax (polyethylene glycol) of known concentration using a syringe. The droplets of Carbowax solution quickly penetrated the bed of particles and formed wet agglomerates. If the bed was kept stationary while adding the droplets, the initial shape of wet agglomerates deviated slightly from spherical due to an uneven penetration of liquid. Shearing the bed at very low rates while adding the droplets helped in achieving an initial nearly spherical shape. The rate and time of shear during this exercise were kept low enough (at about 26 s^{-1} and 30 s. respectively) so that negligibly small elongations were produced. The technique worked well for the entire range of concentrations of Carbowax solutions used.

Experiments on deformation and breakup of wet agglomerates were performed in the following manner. The bed was fluidized at minimum fluidization conditions

and ten initially spherical wet agglomerates were produced in the manner described above. Adding ten droplets of Carbowax solution to the bed took approximately 15 s. Subsequently, the rotation rate of the inner cylinder was increased to the desired value and held constant for a certain amount of time, characteristic of each experiment. During this time the wet agglomerates deformed to various degrees depending upon the experimental conditions. The rotation rate was then reduced to zero and the bed kept stationary at minimum fluidization conditions for several more minutes. During this time the deformed state of the wet agglomerates was preserved while they slowly dried. The required drying time under these conditions, for the range of concentrations of Carbowax solutions used, was found to be about 50 minutes. Dry agglomerates were then carefully sieved and the elongation parameter, E, determined by measuring the major axis manually using a projection microscope.

Two sets of experiments were performed: one in which the variation of elongation parameter, E, with time was studied for a fixed value of the deformation Stokes number, St_{def}, and another in which the variation of E with St_{def} was studied for a fixed time. The deformation Stokes number, St_{def}, was held constant during the first set of experiments by holding constant the rotation rate of the inner cylinder (which determines the shear rate, $\dot{\gamma}$), and the concentration and temperature of the 20 K Carbowax solution (which influences its viscosity, μ). Actual values of shear rate and viscosity were 34 s^{-1} and 0.55 kg m^{-1} s^{-1}, respectively. The particle size, d_{p_g}, and density, ρ_{p_g}, of the glass particles were taken as their mean values provided by the supplier as 300 μm and 2.46 g cm^{-3}, respectively. The value of St_{def} during these set of experiments was thus estimated from equation (2) as 0.013. Several experiments with run times varying from 1 to 15 minutes, with an increment of 1 minute, were performed (see table 3). During the second set of experiments, run time was fixed at 5 minutes. The deformation Stokes number, St_{def}, was varied in this set of experiments by varying both the rotation rate of the inner cylinder and the concentrations of 20 K Carbowax solution. Seven experimental runs were performed with values of St_{def} varying between 0.0008 and 0.0938 (see table 4).

In order to quantify agglomerate breakage (see the last column in tables 3 and 4), the mass of a dry deformed agglomerate, m_a, was compared to its mass at zero time, m_a^o. The mass at zero time, m_a^o, was estimated by forming ten wet agglomerates in the Couette device, imparting an initial spherical shape to them by the method discussed previously, drying them in that state without any further shearing, and measuring their average mass (the diameter of the original undeformed agglomerate, d_o, was estimated by measuring the average diameter of these agglomerates in two perpendicular directions and then taking their average). Under conditions of low deformation, m_a exhibits a slight increase (about 10% on an average) over its zero shear mass, m_a^o (see third and fifth columns in tables 3 and 4 respectively). This phenomenon can be attributed to the capture of particles by the agglomerate from surrounding granular material when it is sheared. The effect of agglomerate breakage, on the other hand, tends to reduce the dry agglomerate mass, m_a, either as result of chipping of individual particles from the ends along the major axis, or as a result of its fragmentation into two or more agglomerates. A dry agglomerate is thus (quite arbitrarily) considered as 'broken' if its mass, m_a, is less than 90% of its corresponding mass at zero time, m_a^o. The last column in tables 3 and 4 reports the number of unbroken agglomerates, out of the initial ten, as determined by this criterion. The third and fifth columns in tables 3 and 4 list respectively the average ratio m_a/m_a^o measured over the unbroken agglomerates. Measurements of the elongation parameter, E, are also reported as averages over the unbroken agglomerates.

Time (min.)	Elongation parameter (E)	m_a/m_a^o	Number unbroken
1	1.11	1.11	10
2	1.17	1.11	10
3	1.16	1.06	10
4	1.18	1.09	10
5	1.24	0.96	10
6	1.29	1.03	10
7	1.30	1.01	10
8	1.32	0.99	10
9	1.36	0.96	9
10	1.33	0.96	7
11	1.35	1.03	7
12	1.41	0.98	6
13	1.47	1.00	7
14	1.50	0.99	4
15	—	—	0

TABLE 3. Experimental results for the variation of elongation parameter, E, with time for a fixed value of deformation Stokes number, $St_{def} = 0.013$.

Viscosity of Carbowax solution (kg m^{-1} s^{-1})	Shear rate (s^{-1})	Deformation Stokes number (St_{def})	Elongation parameter (E)	m_a/m_a^o	Number unbroken
7.82	31.41	0.000889	1.07	1.22	10
4.52	39.26	0.001923	1.14	1.21	10
2.41	45.55	0.004174	1.18	1.18	10
1.19	49.21	0.009108	1.33	1.14	10
0.54	49.21	0.019839	1.38	1.03	10
0.23	45.55	0.043087	1.32	0.92	6
0.09	39.26	0.093804	—	—	0

TABLE 4. Experimental results for the variation of elongation parameter, E, with deformation Stokes number, St_{def}, for a fixed run time of 5 minutes.

Figure 11 displays experimental results for the variation of elongation parameter, E, with time for a fixed value of $St_{def} = 0.013$. Some samples of dry deformed agglomerates are placed vertically above data points to which they correspond. The elongation parameter, E, is observed to increase with time. The behaviour is in good qualitative agreement with the 'smoothed-out' behaviour of figure 6(c), which displays the simulation results for the variation of E with time, for a fixed value of $St_{def} = 0.018$. E acquires a value of about 1.1 in 1 minute and increases to a value of about 1.5 in 14 minutes. Partial breakage of agglomerates (only some of the original ten surviving) is observed for all times exceeding 8 minutes. The fraction of broken agglomerates increases with time, and all agglomerates break during the experiment with a run time of 15 minutes.

Though the values of St_{def} in experimental and simulation conditions of figures 11 and 6(c) are close, there is a substantial disparity in run times. The simulation run time in figure 6(c) is 200 dimensionless units, whereas the experimental one

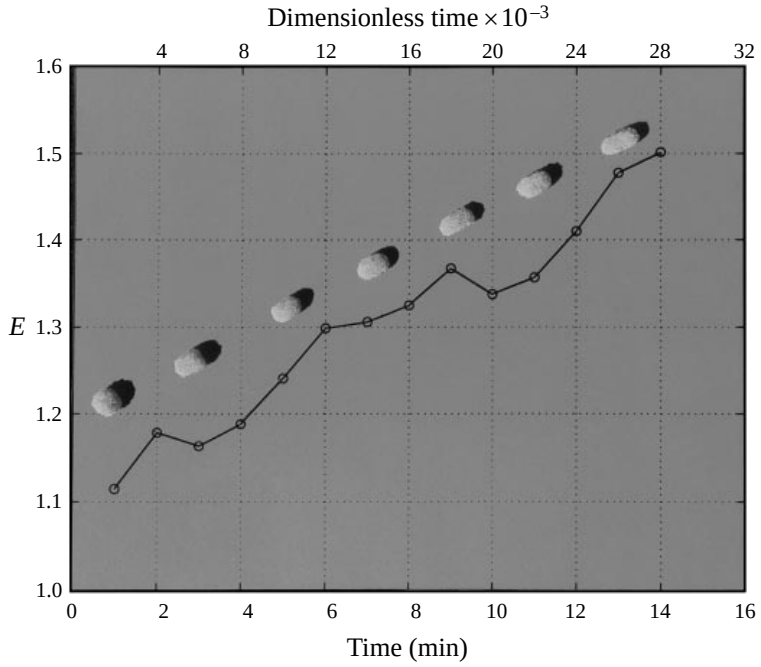

FIGURE 11. Variation of the elongation parameter, E, with time for a constant value of deformaton Stokes number, $St_{def} = 0.013$.

in figure 11 ranges from about 2042 to 28 588 dimensionless units (from 1 to 14 minutes). Much larger run times are required in actual experiments since variations in E can be measured accurately over small time increments in simulations but cannot be measured accurately in experiments, due to the presence of experimental 'noise'. Meaningful data in experiments can be gathered only over time increments of about 1 minute, which, at the experimental conditions in the apparatus, corresponds to about 2042 dimensionless time units.

Figure 12 displays experimental results for the variation of the elongation parameter, E, with the deformation Stokes number, St_{def}, for a fixed run time of 5 minutes. Samples of dry deformed agglomerates are again placed vertically above the data points to which they correspond. E is observed to increase with St_{def}. The two regimes of low and high characteristic deformation are also apparent. The behaviour is again in good qualitative agreement with that of figures 8 and 9, which display the simulation results for the variation of E with St_{def} for various dimensionless time units and relative agglomerate diameters (d_a/d_p). Values of d_a/d_p, ranged in simulations from about 10.9 to 27.3, and in experiments from about 16.8 (for an agglomerate made of 50% Carbowax solution) to about 22.6 (for an agglomerate made of 25% Carbowax solution).

The lower limit of St_{def} in figure 12 is chosen such that a sufficiently low value of E is obtained within the given experimental run time. The increment in the value of St_{def}, by a factor of $10^{1/3}$ between two successive data points, is again chosen such that a clear pattern of change in E with St_{def} is observed. The upper limit is determined by the lowest possible concentration of Carbowax solution which can still make agglomerates strong enough so that they do not break easily during handling. The

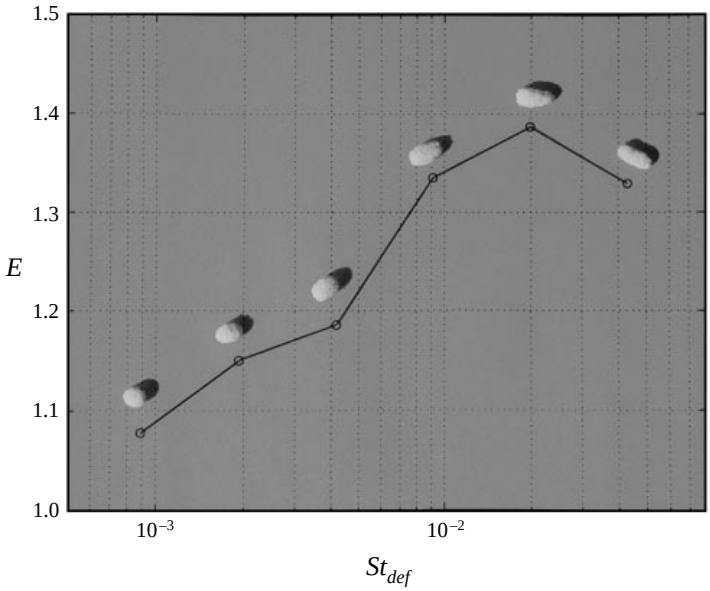

FIGURE 12. Variation of elongation parameter E with the deformation Stokes number, St_{def}, for a constant run time of 5 minutes.

run time of 5 minutes is taken such that for the chosen range of St_{def}, agglomerates in the high-elongation regime acquire a sufficiently high elongation without breaking.

A quantitative comparison of the values of the critical Stokes number, St^*_{def}, in experiments and simulations can be made despite the fact that simulations and experiments cover different time ranges, since St^*_{def} was observed in figure 8 to be relatively insensitive to the variations in time. The value of St^*_{def} from experimental results of figure 12 is estimated approximately as 0.006. The same critical value estimated from simulation results in figures 8 and 9 was found to be approximately 0.02. The discrepancy is surprisingly small considering experimental error, the large number of assumptions in the simulation model and the fact that the simulation is two-dimensional while the experiments are not. Partial breakage of agglomerates is observed for the run corresponding to $St_{def} = 0.043$ ($St_{def} > St^*_{def}$). A run corresponding to $St_{def} = 0.093$ ($St_{def} \gg St^*_{def}$) resulted in a breakage of all agglomerates, as expected.

6. Conclusions

In addition to providing insight into the phenomenon of shear-induced agglomerate deformation and breakup, the analysis presented in this paper provides a new means of theoretical modelling of granulation. Conditions during granulation under which the agglomerates break are important in defining their mean size. In view of the present analysis, this breakup can be characterized by means of the deformation Stokes number, St_{def}, of the system. A magnitude of St_{def} below its critical value, St^*_{def}, would imply low breakup forces, and vice versa. Under conditions of high enough shear, such that when the limit of breakup is met for all agglomerates, a simple estimate of the equilibrium operating point may be obtained by equating the deformation Stokes number, St_{def}, of the system, based upon the average agglomerate properties, to its critical value, St^*_{def}. Taking St^*_{def} as a constant property of the system

in the spirit of the present computations, and as a first approximation equating it to its computed or experimentally determined value, one can arrive at an approximate interdependence of various operating parameters at steady state. All other parameters being constant, such an analysis yields an inverse dependence of the square of the agglomerate size on the shear rate.

It is also interesting to compare the present study with that of shear-induced deformation and breakup of viscous drops in viscous fluids (Stone 1994). A drop of viscous fluid when suspended in another viscous fluid undergoing shear flow exhibits a phenomenon identical to that observed in the present study: that of deformation by stretching. In both cases stretching occurs in the direction of the straining component of the shear field (figure 7): whereas the straining component causes the drop/agglomerate to elongate, vorticity in the flow serves to reduce the elongation. In the case of a drop, steady deformed shapes are possible since the surface tension effects drive the flow back into the drop and thus always try to make the drop spherical again. When the outer flow is stopped, the drop would regain its original spherical shape. However, steady deformed shapes in case of agglomerates are not possible because surface tension effects at the interface are negligibly small and there is no force which acts to make an elongated agglomerate spherical again. The mode of fragmentation in the two cases is also different. In the case of a drop, fragmentation of an elongated drop occurs due to an instability in flow, and is caused by surface tension effects. Fragmentation of an elongated agglomerate is caused as a result of narrowing of its smaller dimension to a size comparable to that of the individual particles, and a subsequent rupture of liquid bridges which tend to hold them together.

A better quantitative comparison of the simulation results with experiments requires improvements in the experimental setup and/or a larger CPU time for simulations. A better experimental setup, with larger cylinder diameters to yield reduced curvature effects and one with a better speed control over the rotation of inner cylinder, would serve to reduce the experimental noise. This would allow the collection of data at smaller increments of time and St_{def}, thus also allowing lower total run times. This would hence make comparisons with simulation results at lower times much easier. An increase in the simulation run time on the other hand is limited by the available CPU time. A simulation of 100 dimensionless time units in the present simulation with 10 000 particles required about 3 hours of CPU time on a SGI Power Challenge workstation (using a MIPS R8000 microprocessor). Thus a simulation run for a time comparable to the *smallest* experimental run time (1 minute or 2042 dimensionless time units) would require about 61 hours (2.5 days) of CPU time.

Relaxing the assumptions made in the simulation model also implies requiring larger CPU times. Consider an extension of the present simulation to three dimensions. Assuming a similar particle number density in three dimensions requires a simulation with about 10^6 particles. Since the computational algorithm for N number of particles is $O(N)$ (computation in both granular and agglomerate phases is $O(N)$), a simulation of 100 dimensionless time units on a similar machine would require about 300 hours (12.5 days) of CPU time. Reducing the number of particles would reduce the CPU time but would also increase the error in computation, thus requiring many simulation runs in order to reduce the error. Another appropriate extension to the work would be to incorporate the effect of lubrication forces in the agglomerate phase, which were neglected in computing the dynamics of particle movement in the agglomerate in §2. Computational demands of such an extension are even more severe, since the incorporation of lubrication forces is a costly $O(N^3)$ operation. If we assume that on

an average 10% of particles are occupied by the agglomerate phase, incorporation of lubrication forces in the present simulations would increase the CPU time to about $3((9000 + 1000^3)/10\,000)$ or 3×10^5 hours.

Despite its limitations, the present simulation model has provided a neat description of the process, both qualitatively and quantitatively. Moreover, the experiments have confirmed the qualitative conclusions reached from the simulation results. Together, the simulations and experiments, have led to a much better understanding of the phenomenon of shear-induced deformation and breakup of wet agglomerates, and, at least in principle, have provided the rudiments of a prediction model of granulation.

Simulations in this work were carried out on the computer system SGI Power Challenge Array at the National Center for Supercomputing Applications, University of Illinois at Urbana-Champaign. Helpful discussions with Professor Michel Y. Louge of Cornell University are acknowledged with appreciation. Zhen Rong Xu, Ivan Ortiz and Andrew Eng helped with the construction of the experimental setup.

REFERENCES

Aidanpää, J. O., Shen, H. H. & Gupta, R. B. 1996 Experimental and numerical studies of shear layers in granular shear cell. *J. Engng Mech. ASCE* **122**, 187–196.

Bossis, G. & Brady, J. F. 1984 Dynamic simulation of sheared suspensions. I. General method. *J. Chem. Phys.* **80**, 5141–5154.

Bouillot, J. L., Camoin, C., Belzons, M., Blanc, R. & Guyon, E. 1982 Experiments on 2-D suspensions. *Adv. Colloid Interface Sci.* **17**, 299–305.

Brady, J. F. & Bossis, G. 1985 The rheology of concentrated suspensions of spheres in simple shear flow by numerical simulation. *J. Fluid Mech.* **155**, 105–129.

Brady, J. F. & Bossis, G. 1988 Stokesian dynamics. *Ann. Rev. Fluid Mech.* **20**, 111–157.

Campbell, C. S. 1989 The stress tensor for simple shear flows of a granular material. *J. Fluid Mech.* **203**, 449–473.

Campbell, C. S. 1990 Rapid granular flows. *Ann. Rev. Fluid Mech.* **22**, 57–92.

Campbell, C. S. & Brennen, C. E. 1985 Computer simulation of granular shear flows. *J. Fluid Mech.* **151**, 167–188.

Ennis, B. J., Tardos, G. & Pfeffer, R. 1991 A microlevel based characterization of granulaton phenomena. *Powder Technol.* **65**, 257–272.

Happel, J. & Brenner, H. 1973 In *Low Reynolds Number Hydrodynamics.* Nijhoff, Dordrecht.

Hopkins, M. A. & Louge, M. Y. 1990 Inelastic microstructure in rapid granular flows of smooth disks. *Phys. Fluids* A **3**, 47–57.

Ichiki, K. & Hayakawa, H. 1995 Dynamical simulation of fluidized beds: Hydrodynamically interacting granular particles. *Phys. Rev.* E **52**, 658–670.

Koch, D. L. 1990 Kinetic theory for a monodisperse gas-solid suspension. *Phys. Fluids* A **2**, 1711–1723.

Kunii, D. & Levenspiel, O. 1991 In *Fluidization Engineering*, 2nd Edn. Butterworth-Heinemann.

Pietsch, W. 1996 Successfully use agglomeration for size enlargement. *Chem. Engng Prog.* **92**, 29–45.

Savage, S. B. & Sayed, M. 1984 Stresses developed by dry cohesionless granular materials sheared in an annular shear cell. *J. Fluid Mech.* **142**, 391–430.

Simons, S. J. R. 1996 Modelling of agglomerating systems: from spheres to fractals. *Powder Technol.* **87**, 29–41.

Simons, S. J. R., Seville, J. P. K. & Adams, M. J. 1994 An analysis of the rupture energy of pendular liquid bridges. *Chem. Engng Sci.* **49**, 2331–2339.

Stone, H. A. 1994 Dynamics of drop deformation and breakup in viscous fluids. *Ann. Rev. Fluid Mech.* **26**, 65–102.

Walton, O. R. & Braun, R. L. 1986 Stress calculations for assemblies of inelastic spheres in uniform shear. *Acta Mechanica* **63**, 73–86.